Title	Smooth C(alkyl)-H Bond Activation in Rhodium Complexes Comprising Abnormal Carbene Ligands
Authors(s)	Krüger, Anneke, Häller, Jonas, Müller-Bunz, Helge, Albrecht, Martin, et al.
Publication date	2011-10-14
Publication information	Krüger, Anneke, Jonas Häller, Helge Müller-Bunz, Martin Albrecht, and et al. “Smooth C(Alkyl)-H Bond Activation in Rhodium Complexes Comprising Abnormal Carbene Ligands.” Royal Society of Chemistry, October 14, 2011. https://doi.org/10.1039/C1DT11116G.
Publisher	Royal Society of Chemistry
Item record/more information	http://hdl.handle.net/10197/6664
Publisher's version (DOI)	10.1039/C1DT11116G

Smooth C(alkyl)–H bond activation in rhodium complexes comprising abnormal carbene ligands

Anneke Krüger,[a] L. Jonas L. Häller,[b] Helge Müller-Bunz,[a] Olha Serada,[c] Antonia Neels,[c] Stuart A. Macgregor*[b] and Martin Albrecht*[a]

Received (in XXX, XXX) Xth XXXXXXXXX 200X, Accepted Xth XXXXXXXXX 200X
First published on the web Xth XXXXXXXXX 200X
DOI: 10.1039/b000000x

Rhodation of trimethylene-bridged diimidazolium salts induces the intramolecular activation of an alkane-type C–H bond and yields mono- and dimetallic complexes containing a formally monoanionic *C,C,C*-tridentate dicarbene ligand bound to each rhodium centre. Mechanistic investigation of the C_{alkyl}–H bond activation revealed a significant rate enhancement when the carbene ligands are bound to the rhodium centre via C4 (instantaneous activation) as compared to C2-bound carbene homologues (activation incomplete after 2 days). The slow C–H activation in normal C2-bound carbene complexes allowed intermediates to be isolated and suggests a critical role of acetate in mediating the bond activation process. Computational modelling supported by spectroscopic analyses indicate that halide dissociation as well as formation of the agostic intermediate is substantially favoured with C4-bound carbenes. It is these processes that discriminate the C4- and C2-bound systems rather than the subsequent C–H bond activation, where the computed barriers are very similar in each case. The tridentate dicarbene ligand undergoes selective H/D exchange at the C5 position of the C4-bound carbene exclusively. A mechanism has been proposed for this process, which is based on the electronic separation of the abnormal carbene ligand into a cationic N–C–N amidinium unit and a metalla-allyl type M–C–C fragment.

Introduction

The selective activation of inert bonds, in particular C–H bonds in alkanes and related compounds, has significant implications in many different areas of chemistry.[1] Foremost, mild routes to C_{alkyl}–H bond activation provide access to unprecedented retrosynthetic opportunities in organic synthesis[2] and yield highly desirable processes for a more efficient fossil fuel utilisation.[3] Although promising advances have been made in homogeneous transition metal-mediated activation of unfunctionalised C–H bonds,[4] drawbacks persist such as the limited substrate scope, or the harsh reaction conditions required to achieve substantial turnover frequencies, and industrial processes are relatively rare.[5]

Two major pathways have been put forward for C_{alkyl}–H bond activation,[4f,4i,6] and they involve either (complex-assisted) σ-bond metathesis[7] or oxidative additions.[8] The former is perhaps most prominently illustrated with Hartwig's rhodium(III) catalyst for mild and selective alkane borylation.[9] Most other alkane activation catalysts operate, however, along the oxidative addition route and include the insertion of a metal centre into the C–H bond.[4] Recent calculations have suggested that the metal centre for oxidative addition may be either nucleophilic, electrophilic, or amphiphilic.[10] A further variation is ambiphilic metal-ligand assisted (AMLA) C_{alkyl}–H bond activation involving chelating bases, and this is thought to be widely operative in synthesis.[11]

A conceivable approach to develop new systems for (catalytic) C_{alkyl}–H bond activation thus consists of using electron-rich transition metals that are bound by strong electron donor ligands, thus providing a high level of nucleophilicity to promote C–H oxidative addition. Ligands derived from N-heterocyclic carbenes (NHCs) may be particularly useful spectator ligands for such application, as NHCs entail high σ-basicity and low π-acidity paired with a rather covalent bonding to the metal centre.[12] Late transition metals comprising NHC ligands have indeed been reported to activate unreactive bonds.[13] Further enhancement of the donor ability imparted by the NHC ligand may be achieved upon changing the ligand coordination. Substantially stronger donor properties were noted for NHCs bound via C4 rather than C2,[14] often referred to as abnormal bonding.[15] In this coordination mode, the metal-bound carbon experiences a lower σ-withdrawing effect due to the presence of only one nitrogen atom in the α position. Indeed, abnormally bound carbene complexes have shown intriguing catalytic activity in bond activation processes, surpassing in many instances that of normal carbene analogues.[16] Within this context, we recently communicated the smooth intramolecular activation of an alkane-type C–H bond in a rhodium complex featuring abnormally bound NHC ligands.[17] Upon expanding on these studies we have identified key parameters that govern the C–H bond activation step. Bond activation in these abnormal carbene complexes presumably is a chelate-assisted process, thus disclosing an additional feature of this particular ligand.

Results and Discussion

C–H bond activation in C2-substituted diimidazolium salts

Reaction of the trimethylene-linked diimidazolium salts **1** with hydrated $RhCl_3$ in the presence of NaOAc yielded the

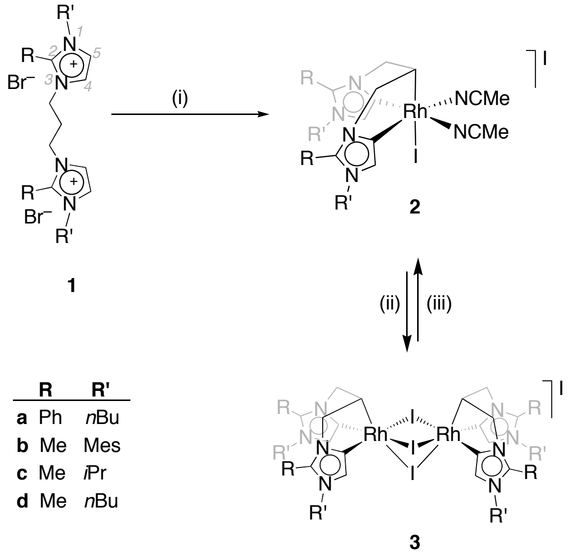

Scheme 1 Metallation of a trimethylene-linked diimidazolium salt: (i) $RhCl_3$, NaOAc, MeCN (reflux), then KI; (ii) CH_2Cl_2, RT; (iii) MeCN, RT

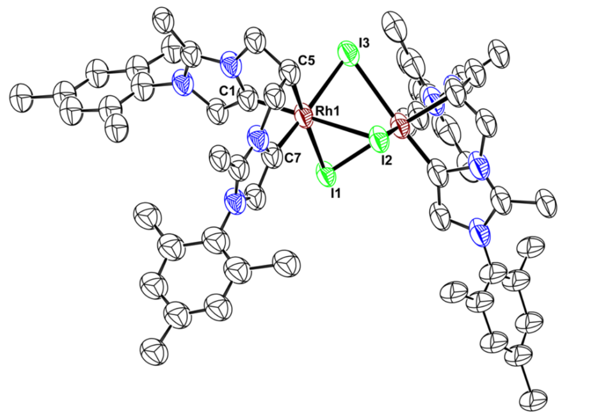

Fig. 1 Ortep representation of the cationic portion of **3b** (30% probability). Hydrogen atoms and co-crystallised solvent atoms have been omitted for clarity. Selected bond lengths (Å): Rh1–C1 1.974(17), Rh1–C7 1.939(18), Rh1–C5 2.075(15), Rh1–I1 2.8052(16), Rh1–I2 2.7808(17), Rh1–I3 2.7934(19). Selected bond angles (deg): C1–Rh1–C7 85.6(7), C1–Rh1–C5 83.4(6), C5–Rh1–C7 84.1(7), C1–Rh1–I2 174.1(5), C5–Rh1–I1 178.0(5), C7–Rh1–I3 175.4(5); the environment around the Rh2 centre is similar.

tridentate dicarbene complexes **2**, and after column chromatography the dimetallic complexes **3** (Scheme 1). Formation of **2** implies a triple C–H bond activation process including activation of the alkyl C–H bond in the linker in addition to the expected[18] heterocyclic C–H bond activation. The activation of the linker occurred under relatively mild conditions, *i.e.* in moist MeCN at 82 °C and in an aerobic atmosphere. Variation of the substituents within the heterocycle (aryl *vs* alkyl group at C2 and N1, bulky *i*-Pr *vs* linear alkyl groups at N1) did not have a significant effect on the bond activation process and the ligand consistently adopted a tridentate bonding mode. No intermediate was detected when stopping the reaction at low conversion. Hence the aliphatic C–H bond activation is a general process, provided the rhodium centre is bound by abnormal carbene ligands. An abnormal bonding mode is enforced in **1a–d** by protection of the imidazolium C2 position.

Formation of either the monometallic complexes **2** or the dimetallic complexes **3** was dependent on the coordination ability of the solvent. Purification of the complexes by column chromatography using CH_2Cl_2 and acetone as eluents gave the dimetallic species **3**, whereas addition of MeCN afforded the monometallic complexes **2** exclusively. All monomeric complexes displayed two sets of ^{1}H NMR signals in solution (CD_3CN), which have been attributed to two isomers featuring the iodide ligand *trans* to the alkyl ligand and *trans* to one of the carbene ligands, respectively. Generally, the signals appear in approximate 2:1 ratio, which indicates a statistical distribution of the iodide ligand over all three available positions, and thus a similar *trans* influence of the abnormal carbene and alkyl ligands. In all complexes but **2b**, the major isomer of **2** revealed significant broadening of the carbene resonances both in the ^{1}H and ^{13}C NMR spectra, while in the minor species, the trimethylene resonances were broad. This behaviour was assigned to fluxional coordination of the iodide ligand, either *trans* to one of the carbene ligands (major isomer) or *trans* to the alkyl ligand (minor isomer). In complex **2b** the ratio is inverted (1:1.2) with the major species featuring a well-resolved carbene resonance at δ_C 146 ($^1J_{RhC}$ = 46 Hz), while the minor species, attributed to the isomer with a mutual *cis* arrangement of iodide and alkyl ligands, displays broad carbene signals and a sharp doublet for the rhodium-bound alkyl carbon (δ_C 34.0, $^1J_{RhC}$ = 28.5 Hz). For the dimeric complexes **3**, two major sets of signals in approximately 2:1 ratio were identified by NMR spectroscopy. These sets were tentatively assigned to *syn* and an *anti* eclipsed conformations of the two tridentate ligands. The protons of the trimethylene linker and likewise the NCH_2 protons of the butyl wingtip groups in **3a** and **3d** are diastereotopic, in line with a hindered rotation about the Rh–C bonds.[19]

The dimeric structure of **3b** was unambiguously confirmed by an X-ray diffraction analysis of a single crystal that was grown after exchange of the non-coordinating anion from I^- to PF_6^-. The molecular structure is almost C_{2v}-symmetric (Fig. 1). The $C_{carbene}$–Rh–$C_{carbene}$ bite angles of the two crystallographically independent sites are slightly different (85.6(7)° and 89.7(8)° respectively), which suggests some steric flexibility of the chelate. As reported previously for **3c**,[17] the Rh–$C_{carbene}$ bonds are substantially shorter than the Rh–C_{alkyl} bonds (average 1.94(3) *vs* 2.074(1) Å), yet the Rh–I bonds are all similar (average Rh–I 2.80(2) Å). These data suggest similar *trans* influences of alkyl and carbene ligands, in line with the statistical mixture of isomers found in solution (see above).

Normal and mixed normal-abnormal dicarbene complexes

In order to evaluate effects that are critical for inducing the smooth C_{alkyl}–H bond activation observed during the formation of **2** and **3**, rhodation of ligand precursor **1e** was investigated in more detail (Scheme 2). In this precursor, the imidazolium C2-positions are not protected and hence available for metal coordination via the normal carbene coordination mode. Upon exposure of **1e** to identical conditions as the diimidazolium salts **1a–d**, *i.e.* hydrated $RhCl_3$ and NaOAc in refluxing MeCN, a mixture of products

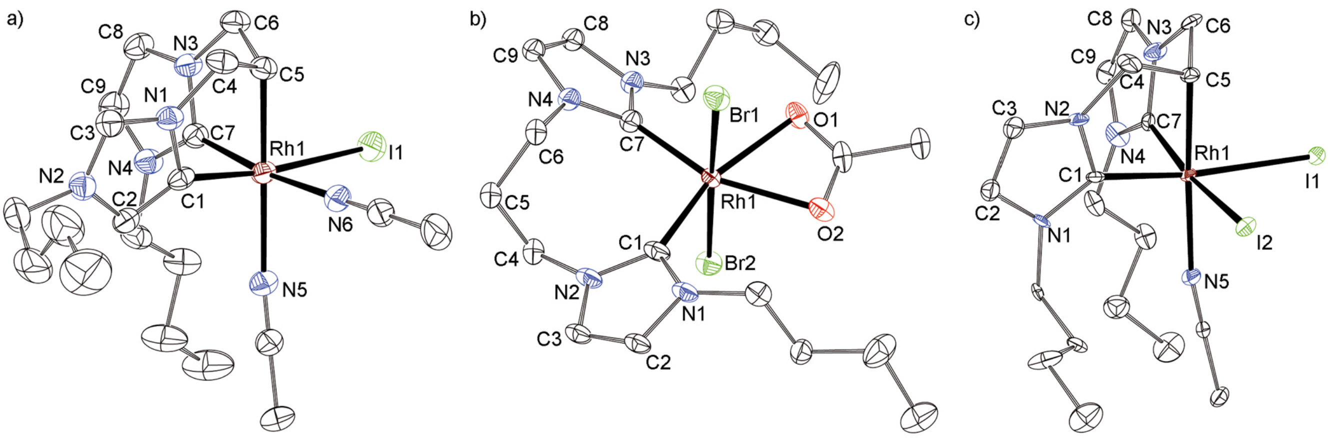

Fig. 2 ORTEP representation of the cationic complex **4** (a; 40% probability), neutral dicarbene complex **5b** (b; 50% probability), and the neutral tridentate complex **6** (c; 50% probability). Hydrogen atoms and non-coordinating iodide in **4** omitted for clarity.

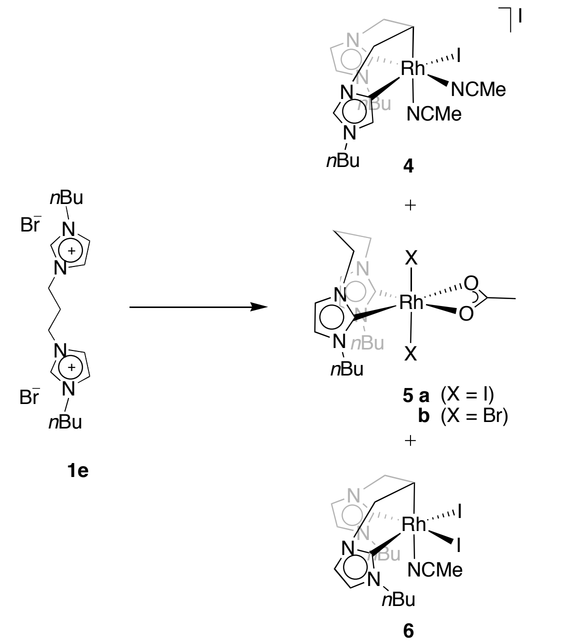

Scheme 2 Metallation of **1e**. Reagents and conditions: $RhCl_3$, NaOAc, MeCN (reflux), then KI (for **4**, **5a**, and **6**) or KBr (for **5b**).

was obtained after 16 h (Scheme 2). Complex **5** was isolated from this mixture in 21% yield after column chromatography. This complex features a bidentate coordinated ligand with both carbenes in the normal bonding mode; a close analogue was previously reported by Peris and coworkers.[19a]

Careful analysis of the reaction mixture before chromatographic separation revealed, in addition to **5**, also the presence of the tridentate biscarbene complexes **4** and **6**, both resulting from C_{alkyl}–H bond activation. In complex **4** the tridentate ligand features an abnormally and a normally bound carbene, whereas in complex **6** both carbenes are in the normal bonding mode. All three complexes were isolated by fractional crystallisation and were fully characterised by X-ray crystallography and NMR spectroscopy.

Complexes **4**, **5b**, and **6** all crystallised as monomers with the rhodium centre in a slightly distorted octahedral environment (Fig. 2). Like in complex **3**, the Rh–$C_{carbene}$

Table 1 Selected bond lengths and angles for complexes **4**, and **5b**, and **6**

	4	5	6
Rh1–C1	1.995(3)	1.978(10)	1.995(8)
Rh1–C7	1.962(3)	1.970(8)	1.988(8)
Rh1–C5	2.071(3)	---	2.063(8)
C1–Rh1–C7	85.07(11)	98.9(4)	91.5(3)
C1–Rh1–C5	82.81(11)	---	80.6(3)
C5–Rh1–C7	81.59(11)	---	81.7(3)

[a] bond lengths in Å, bond angles in deg.

bonds in complexes **4** and **6** are significantly shorter than the Rh–C_{alkyl} bonds. The normal carbene ligand in **4** is *trans* to a MeCN ligand and is closer to the rhodium centre (Rh–C7 1.962(3) Å) than the abnormal carbene ligand (Rh–C1 1.995(3) Å). Longer Rh–$C_{carbene}$ bonds were also noted for the all-normal carbene complex **6** (Rh–$C_{carbene}$ 1.995(8) and 1.988(8) Å), where the carbenes are positioned *trans* to iodide, which has a stronger *trans* influence than MeCN.[20]

The dicarbene bite angle in complex **5b** is unusually large, C1–Rh1–C7 is 98.9(4)°,[19–21] and the dihedral angle between the imidazolylidene rings and the metal *xy* coordination plane (defined by C1, Rh1, and C7) is much smaller (20.8–29.0°) than in the tridentate complex **4**, where the heterocycles are positioned nearly perpendicularly (dihedral angle between 80.9° and 84.6°). The conformational flexibility of the ligand imparted by the flexible trimethylene linker is further illustrated by the synrotatory twisted arrangement of the imidazolylidene rings, thus avoiding steric congestion and yielding a propeller-like arrangement rather than the generally observed V-shaped conformation.[19] Steric considerations may also account for the mutual *trans* arrangement of the iodide and one carbene ligand in complexes **4** and **6**.

Even though complexes **4** and **6** have a related tridentate ligand, only complex **6** contains a formally neutral rhodium centre while complex **4** is monocationic. The stabilisation of a formally cationic rhodium centre in **4** may be a direct consequence of the larger mesoionic character of the C4-bound imidazolylidene ligand as compared to the normal analogue in **6**,[22] thus illustrating the stronger donor power of the abnormal carbene.[14,23] Bond length analysis in the heterocycles suggests a vinyl-type bonding of the C4-bound carbene ligand in **4**, including remote charge stabilisation by the cationic amidinium fragment.

In solution, complex **4** displays a complicated ^{1}H NMR signal pattern that simplifies upon heating to 60 °C. At this elevated temperature, the inequivalence of the carbene bonding modes is reflected by the presence of four singlet resonances for the imidazolium protons. Most characteristic is the low-field resonance at δ_H 8.31 due to the C2-bound hydrogen of the abnormal carbene residue. The two butyl groups resonate as two disparate sets of signals both in the ^{1}H and ^{13}C NMR spectra. Similarly, the NCH_2 protons of the trimethylene linker appear as two distinct sets of AB doublets, one at δ_H 4.38 and 3.83 ($^{2}J_{HH}$ = 13.0 Hz) and the other at δ_H 4.32 and 3.67 ($^{2}J_{HH}$ = 12.0 Hz). The proton attached to the rhodium-bound carbon is very broad due to the coupling to four inequivalent protons and to the rhodium centre. At room temperature, the presence of three different species were identified to be present from the split of the lowest field singlet into three resonances between 8.4 and 8.2 ppm in approximate 1:4:6 ratio. The presence of three species may be rationalised with rigid iodide coordination at room temperature, either *trans* to the alkyl group or to either of the two different carbene ligands and may thus reflect the different *trans* influence of normally and abnormally bound NHC ligands and the alkyl ligand, respectively.

The NMR spectrum of complex **5b** displays a single set of signals for the imidazolylidene ligands (δ_H 7.61 and 7.41, $^{3}J_{HH}$ = 2.5 Hz), indicating C_s-type symmetry in solution. All N-bound CH_2 protons are diastereotopic and resonate as four sets of multiplets due to the rigid conformation of the metallacycle on the NMR time scale even at elevated temperatures (up to 60 °C).[19] Obviously, the crystallographically deduced C_1 symmetry is not preserved in solution and swinging about the $C_{carbene}$–Rh bond is fluxional.

A similar C_s symmetric conformation was deduced for complex **6** at 70 °C. The aromatic signals of the tridentate ligand are shifted to higher field as compared to the bidentate ligand in **5b** and appear at δ_H 7.15 and 7.03. The C_s symmetry supposedly arises from dissociation of one iodide ligand and fluxional coordination of the second iodide in the formally cationic system (see complex **2** above). Upon lowering the temperature, the structure becomes unsymmetrical and at −10 °C the imidazolium protons resonate as four doublets at δ_H 7.23, 7.08, 7.07 and 6.97 ($^{3}J_{HH}$ = 1.9 Hz). In line with the observed behaviour of complexes **2** and **4**, iodide coordination at lower temperature is surmised to be rigid on the NMR time scale, thus producing an asymmetric cationic complex with the iodide presumably *cis* to the alkyl ligand.[24]

Mechanistic studies

Based on the characteristic ^{1}H NMR signals, it was possible to identify and quantify complexes **4**, **5**, and **6** also in composite mixtures. Since kinetic studies through *in situ* measurements were hampered by the inhomogeneity of the reaction mixture, the progress of the reaction was monitored through ^{1}H NMR measurement of samples taken at regular intervals. A typical plot of the relative concentrations of **4**, **5**, and **6** during the first 12 h of the reaction is shown in Fig. 3. In addition to these three complexes, the reaction mixture was composed of the diimidazolium salt **1e** and presumably some monocarbene species,[25] which could not be confidently identified and quantified in the product mixture.

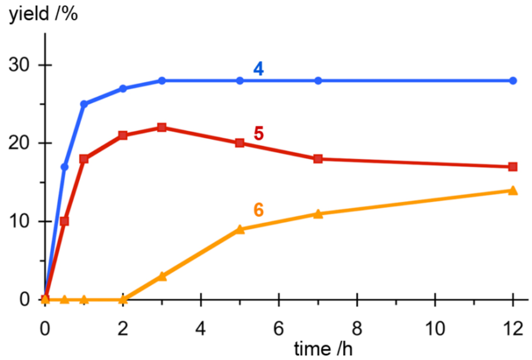

Fig. 3 Time-dependent evolution of **4**, **5** and **6** from the reaction of **1e** with $RhCl_3$ (determined by ^{1}H NMR spectroscopy).

Analysis of the reaction mixture composition allowed key factors to be identified that govern the formation of the different cyclometallated products. Thus, initial production of complex **4** is relatively fast and essentially complete after 2 h. No mono- or bidentate intermediate comprising a C4-bound carbene was observed and the concentration of the tridentate complex did not change any further, even though the reaction mixture contained residual monocarbene species (see below). Only after heating for several days, a slow decrease of the concentration of **4** was observed. This decrease was attributed to complex decomposition, hence revealing a limited long-term stability of this complex at elevated temperatures.

Formation of the bidentate dicarbene species **5** occurred at slightly lower rates than the tridentate complex **4** and preceded the formation of the tridentate complex **6**. Only after about 2 h and significant build-up of **5**, C_{alkyl}–H activation was induced and complex **6** started to appear. The increase of **6** was more pronounced than the apparent consumption of **5**, presumably because of continuous formation of this complex from **1e** or the corresponding monocarbene species. At extended reaction times (12–24 h), the rates for the formation of **6** and the consumption of **5** became essentially equal, yet low. After 60 h, the **5**:**6** ratio is about 1:2, indicating that C_{alkyl}–H bond activation from **5** is very slow and not complete even after several days, thus sharply contrasting the instantaneous bond activation in the formation of **4**.

The data further suggest that formation of **4** and **6** are mutually independent processes and do not result from interconversion of an abnormal carbene bonding mode to a normal one or *vice versa*.[26] However, complexes **5** and **6** seem to be interconnected. Indeed, separate experiments starting from pure **5** revealed a slow C_{alkyl}–H bond activation in the presence of NaOAc in refluxing MeCN, and conversion to **6** occurred over several days. Hence, product selectivity should be biased at an early stage of the reaction, most likely at the initial heterocyclic C–H bond activation process. This model suggests that initial activation of the C4–H in **1e** is energetically not much different from C2–H bond activation. The substantially lower acidity of the C4-bound proton[27] may thus be compensated by steric (de)shielding, suggesting the

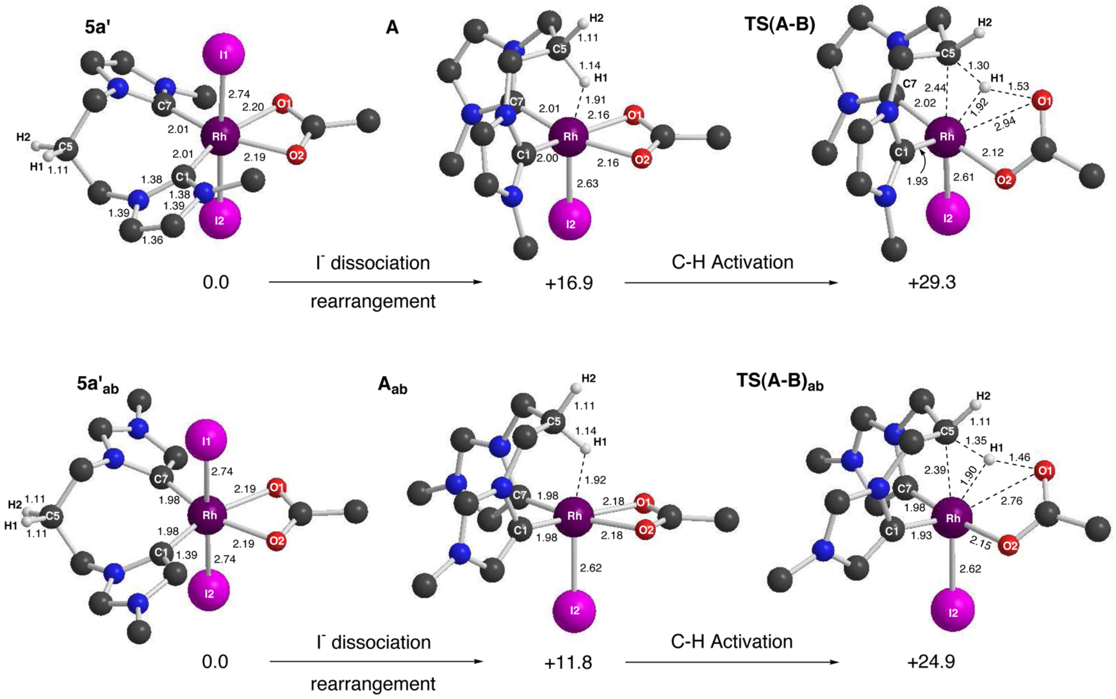

Fig. 4 Computed geometries with selected distances in ångstrom for C–H activation from **5a'** and **5a'$_{ab}$** (H atoms, excepting those of the C5 methylene group, are omitted for clarity). Free energies (kcal mol^{-1}) include a correction for MeCN solvation (PCM method).

product selectivity to be sensitive to wingtip group modifications.[28]

Theoretical analyses

Density functional theory (DFT) calculations employing the BP86 functional have been performed to obtain further insight into how the NHC binding mode affects the C$_{alkyl}$–H bond activation process. Calculations considered the mechanism of C$_{alkyl}$–H bond activation from the key intermediate **5a'** (the prime indicating use of the N–Me analogue of complex **5** used experimentally) and its abnormal NHC analogue **5a'$_{ab}$**, *i.e.* the presumed precursor of complex **2** (Fig. 4). The computed structure of **5a'** compares well with the experimental structure of **5b**; in particular the large bidendate angle (C1–Rh–C7 = 99.8°) and the propeller arrangement of the ligand are correctly reproduced. These features are also apparent in the computed structure of **5a'$_{ab}$** in which the C1–Rh–C7 angle is slightly larger (102.1°) and the Rh–C distances slightly shorter (average 1.98 Å *cf.* 2.01 Å in **5a'**). The remaining Rh–ligand bond distances are very similar in the two structures.

One possible pathway for C$_{alkyl}$–H activation in **5a'** and **5a'$_{ab}$** is shown in Figure 4 and involves initial iodide dissociation and rearrangement of the *bis*-NHC ligand to give intermediates **A** and **A$_{ab}$**. Both these species feature an upright orientation of the carbene rings and greatly reduced bidentate chelate angles (**A**: 92°; **A$_{ab}$**: 86.4°). This arrangement allows the C5–H1 bond to engage in agostic bonding with the Rh centre. The strength of these interactions appears to be comparable in **A** and **A$_{ab}$**, as judged by the similar Rh···H1 and C5–H1 distances (*ca*. 1.91 Å and 1.14 Å respectively). The proximity of the agostic C–H bond *cis* to the κ^2-OAc ligand in **A** and **A$_{ab}$** allows these systems to effect C–H activation via an ambiphilic metal-ligand assisted (AMLA) mechanism.[11,29] This proceeds via **TS(A–B)**/**TS(A–B)$_{ab}$** and involves dissociation of one Rh–O bond such that the free acetate arm becomes available as an intramolecular base that can deprotonate the agostic C–H bond. **TS(A–B)$_{ab}$** displays a slightly later geometry with shorter Rh···C5 and Rh···H1 contacts, somewhat greater C5···H1 elongation and a shorter O1···H1 distance. These C–H activation transition states lead to the 5-coordinated metalated intermediates **B** (E = –0.6 kcal mol^{-1}) and **B$_{ab}$** (E = +1.7 kcal mol^{-1}). The structures of these species closely resemble their preceding transition states, with the full formation of the Rh–C5 bond and proton transfer forming a bound acetic acid molecule (see the ESI for full details).

Figure 4 also shows the relative free energies of the various species implicated in C$_{alkyl}$–H activation, where a correction for the MeCN solvent has also been included via the PCM approach. The overall barrier for C–H activation from **5a'$_{ab}$** is 24.9 kcal mol^{-1}, 4.4 kcal mol^{-1} lower than that for C–H activation from **5a'**. This difference is consistent with the greater reactivity of the abnormal NHC systems towards C$_{alkyl}$–H activation seen experimentally for complexes **2** and **4**. Perhaps surprisingly, however, the origin of this difference does not lie in the C$_{alkyl}$–H activation step itself, where a slightly lower barrier is actually computed from intermediate **A** (12.4 kcal mol^{-1} *cf.* 13.1 kcal mol^{-1} from **A$_{ab}$**). Instead it is the greater ease of iodide dissociation and rearrangement to form the agostic intermediate, lower by 5.1 kcal mol^{-1}, which is responsible for the reduced overall barrier in the C4-bound NHC system. To probe the reasons for this difference we computed the alternative forms of **A** and **A$_{ab}$** where the NHC ligands maintain the conformations seen in **5a'** and **5a'$_{ab}$**. The energies of these species, +13.3 kcal/mol and +10.2 kcal/mol respectively, show iodide dissociation is *ca*. 3 kcal mol^{-1} easier in the C4-bound NHC system. The subsequent rearrangement is also slightly more facile in this case and contributes to the 5.1 kcal mol^{-1} overall difference in the formation of **A** and $\mathbf{A_{ab}}$. This latter component may reflect a greater donation from C4-bound NHC and hence the more effective stabilisation of the agostic intermediate. While this is not particularly apparent in **5a'** and $\mathbf{5a'_{ab}}$, where the Rh–I distances and even the Rh–O distances (*trans* to the NHC ligands) are very similar, the Rh–O distances in $\mathbf{A_{ab}}$ are ca. 0.02 Å longer than in **A**. Trends in the computed natural charges also suggest greater donation from the NHC upon iodide loss. For **5a'** the computed charge on Rh is +0.367 and is actually less positive than the value of +0.384 in $\mathbf{5a'_{ab}}$. In contrast, for intermediate **A** the charge on Rh increases to +0.389, whereas in $\mathbf{A_{ab}}$ there is almost no increase in charge on Rh (+0.385). Although these effects are rather subtle they do point to a greater ability of the C4-bound NHC to stabilise the agostic intermediate and that this, together with the enhanced propensity of iodide dissociation, is responsible for promoting the C–H activation reaction in the C4-bound NHC system.[30]

Reactivity and stability of the complexes

Both the bidentate and tridentate complexes **2–6** are remarkably stable towards air, moisture and elevated temperatures. Slow decomposition was only noted when heated to 80 °C for extended periods of time (>3 days). The complexes were also seemingly robust when treated with moderately strong acids such as HOAc and H_3PO_4. However, when treated with deuterated acids such as D_3PO_4 at RT, complexes **2** and **4** were deuterated at the C5 position to give **2**–D_2 and **4**–D, respectively (Scheme 3). The deuteration was monitored by ^{1}H NMR spectroscopy through the disappearance of the C5-bound heterocyclic proton signal (δ_H 6.78 for **2c**) and was confirmed by the appearance of a resonance at the same frequency in the ^{2}H NMR spectrum. No such reaction was observed when the carbene was normally bound as in complexes **5** and **6**. This reactivity pattern is also illustrated by the exclusive monodeuteration of the mixed abnormal/normal dicarbene complex **4**. In this complex, only the C5-bound proton was exchanged in the presence of D_3PO_4 while the more acidic C2-bound proton was stable and remained unaffected. In line with this observation, the methylene-bridged dicarbene complex **7** underwent H/D exchange under identical reaction conditions and gave **7**–D_2 (Scheme 3).

Heterocyclic H/D exchange occurred much slower in complexes **4** and **7** than in **2**. After 1h at room temperature, 85% deuteration was observed in **2** as compared to 33% in **4** (7% in **7**). Moderate warming to 60 ºC accelerated the exchange considerably and reached 72% in **4** after the same reaction time (83% in **7**). Mechanistically, the deuterium incorporation may be strongly related to the isotope exchange observed in free normal carbenes,[31] and may thus involve transient sp^2-to-sp^3 rehybridisation at C5. Rehybridisation of heterocyclic carbon atoms in NHC complexes has precedents[32]

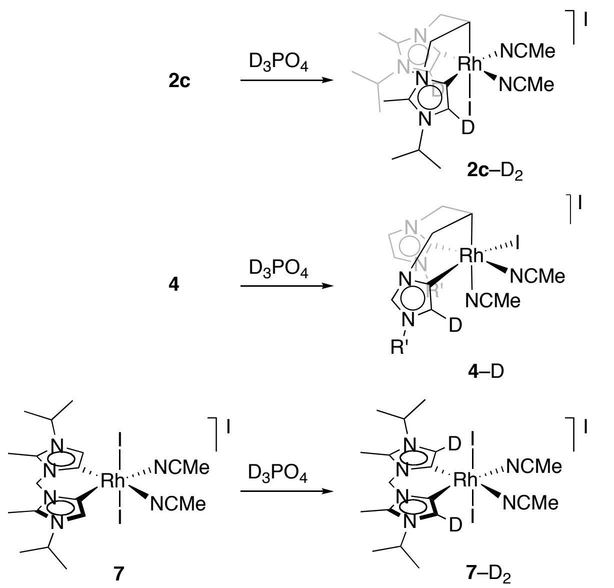

Scheme 3 Reactivity of complexes **2c**, **4**, and **7** towards D_3PO_4.

and may be promoted by the abnormal bonding mode of the carbene, in which contributions from mesoionic resonance structures are more pronounced. In such a limiting structure, the ligand may be separated into a vinylic metal-bound C–C fragment and a N–C–N amidinium cation as charge-compensating unit (Scheme 4).[15b] When bound to the metal, formally a metalla-allyl anion is formed, which may be reversibly protonated either at the metal centre (reinforcing a vinyl-type ligand bonding as in **A**) or at the C5 position (producing a C=Rh carbene complex **B**; Scheme 4). Alternatively, a 1,3-sigmatropic shift of the metal-bound hydrogen to C5 may allow for accessing intermediate **B** from **A**, which upon unselective deprotonation would rationalise the observed H/D exchange at C5. In an attempt to verify this hypothesis, complex **2c** was treated with MeOTf (5 equiv.), which should lead to irreversible C–C bond formation at the imidazolylidene C5 position. When following the reaction at room temperature by ^{1}H NMR using 4,4'-dimethylbiphenyl as internal standard, significant decomposition of the complex was observed after 30 minutes. Presumably, complex degradation was induced by the formation of triflic acid, which may originate from H^+/CH_3^+ substitution at C5.[33] Independent measurements revealed that the carbene

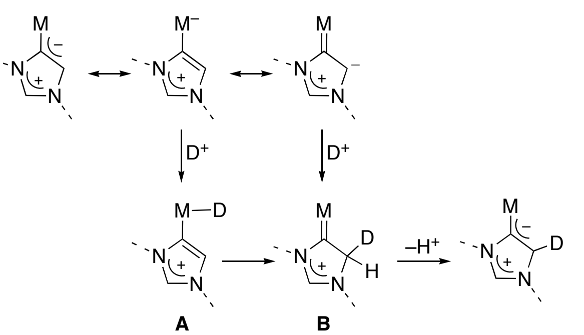

Scheme 4 Proposed mechanism for H/D exchange in abnormal carbene metal complexes.

complex **2c** is indeed instable towards such a strong acid. Performing the reaction in the presence of 1,8-bis(dimethylamino)naphthalene as proton-sponge did not completely prevent decomposition, yet a selective decrease of the signal due to the C5-bound proton to 32% with respect to the other ligand signals was noted, indicating a substantial degree of deprotonation. Although the aliphatic region of the spectrum was rather complicated, a new resonance appearing at δ_H 2.60 and integrating for three protons was tentatively attributed to the C5-methlyated analogue of **2c**. These results point to a cooperative mode of action of the complex, involving the metal centre and the abnormal carbene for bond activation.[34] Such cooperativity may be key for the smooth C–H activation in complexes containing abnormal carbenes as opposed to analogues with normally bound carbenes only.

Conclusions

The intramolecular C_{alkyl}–H bond activation mediated by rhodium carbene complexes has been investigated by using both C2-alkylated and C2-protonated diimidazolium salt precursors. These studies revealed that the activation of both the second heterocyclic C–H bond and in particular the alkyl C–H bond require less energy and proceed at significantly faster rates when the rhodium centre is ligated by an abnormally bound, strongly electron-donating carbene ligand. Specifically C2-protected diimidazolium salts, where the abnormal binding mode is enforced, undergo smooth C_{alkyl}–H bond activation and yield tridentate complexes at ambient temperatures. Theoretical analyses suggest that the ease of formation of the agostic precursors to C–H activation discrimates the two systems. This results from a combination of more facile iodide dissociation in the abnormally bound carbene complexes, presumably due to the pronounced mesoionic character of C4-bound imidazolylidenes, and the ensuing stabilisation of agostic intermediates. Subsequent chelate-assisted C–H bond activation entails similar barriers of *ca*. 13 kcal/mol in each case.

In the presence of mild acids, selective H/D exchange at the abnormally bound carbene heterocycle was observed. This reactivity pattern may be general for C4-bound imidazolylidenes and related ligand systems such as C4-bound 1,2,3-triazolylidenes and may constitute a new pathway for cooperating metal-centred reactivity. Accordingly, these abnormal carbene ligands may act as transient proton acceptors through their mesoionic resonance form, thus transforming the metal-bound carbanion to a formally neutral carbene donor site comprising a remote cationic residue. Preliminary work in our laboratories suggests that this type of metal-ligand cooperativity is general and applicable for the activation of different E–H bonds.

Experimental Section

General comments

The 1,2-disubstituted imidazoles[35] and compounds **1e**, **2c-d**, **5**, and **7** were prepared according to previously reported procedures.[17–19] All other reagents are commercially available and were used as received. Unless otherwise stated NMR spectra were recorded at 25 °C on Bruker and Varian spectrometers operating at 400, 500 or 600 MHz (^{1}H NMR) and 100, 125 or 150 MHz (^{13}C{^{1}H} NMR), respectively. Chemical shifts (δ in ppm, coupling constants J in Hz) were referenced to residual solvent resonances. Assignments are based on homo- and heteronuclear shift correlation spectroscopy. Elemental analyses were performed by the Microanalytical Laboratory at the Federal Institute of Technology in Zurich, Switzerland and at the University College Dublin, Ireland.

Syntheses of 1a

A solution of 2-phenyl *N*-*n*-butyl imidazole (3.47 g, 17.3 mmol) and 1,3-dibromopropane (1.75 g, 8.7 mmol) was stirred in refluxing toluene (20 mL) for 16 h. The formed precipitate was isolated by centrifugation, washed with toluene, and recrystallised from CH_2Cl_2/Et_2O to yield **1a** as an off-white solid (3.12 g, 60%). ^{1}H NMR (CD_3CN, 500 MHz): δ 7.94 (d, 2H, $^3J_{HH}$ = 2.5 Hz, H_{imi}), 7.75 (t, 2H, $^3J_{HH}$ = 7.5 Hz, H_{aryl}), 7.66 (t, 4H, $^3J_{HH}$ = 7.5 Hz, H_{aryl}), 7.55 (m, 3H, H_{aryl}, H_{imi}), 3.97 (t, 4H, $^3J_{HH}$ = 7.5 Hz, $NCH_2CH_2CH_2N$), 3.89 (t, 4H $^3J_{HH}$ = 7.5 Hz, $NCH_2CH_2CH_2CH_3$), 2.16 (quintet, 2H, $^3J_{HH}$ = 7.5 Hz, $NCH_2CH_2CH_2N$), 1.65 (quintet, 4H, $^3J_{HH}$ = 7.5 Hz, $NCH_2CH_2CH_2CH_3$), 1.19 (sextet, 4H, $^3J_{HH}$ = 7.5 Hz, $NCH_2CH_2CH_2CH_3$), 0.78 (t, 6H, $^3J_{HH}$ = 7.5 Hz, $NCH_2CH_2CH_2CH_3$). ^{13}C{^{1}H} NMR (CD_3CN, 125 MHz): δ 145.5 (NCN), 133.7 (C_{aryl}H), 131.5 (C_{aryl}H), 130.8 (C_{aryl}H), 123.3 (C_{imi}), 123.0 (C_{imi}), 122.1 (C_{aryl}), 49.4 ($NCH_2CH_2CH_2CH_3$), 46.3 ($NCH_2CH_2CH_2N$), 32.3 ($NCH_2CH_2CH_2CH_3$), 30.9 ($NCH_2CH_2CH_2N$), 20.0 ($NCH_2CH_2CH_2CH_3$), 13.5 ($NCH_2CH_2CH_2CH_3$). HR-MS (ESI$^+$): Calc. for $C_{29}H_{38}BrN_4$ ([M − Br]$^+$): 521.2280. Found: 521.2280. Anal. calc. for $C_{29}H_{38}Br_2N_4$ (602.45) × H_2O: C, 56.14; H, 6.50; N, 9.03. Found: C, 56.12; H, 6.47; N, 9.00.

Syntheses of 1b

According to the procedure described for **1a**, compound **1b** was obtained from 2-methyl *N*-mesityl imidazole (1.20 g, 6.0 mmol) and 1,3-dibromopropane (0.61 g, 3.0 mmol) as an off-white solid (1.52 g, 73%). ^{1}H NMR (CD_3CN, 500 MHz): δ 8.18 (d, 2H, $^3J_{HH}$ = 2.0 Hz, H_{imi}), 7.36 (d, 2H, $^3J_{HH}$ = 2.0 Hz, H_{imi}), 7.14 (s, 4H, H_{mes}), 4.55 (t, 4H, $^3J_{HH}$ = 8.0 Hz, $NCH_2CH_2CH_2N$), 2.66 (m, 2H, $NCH_2CH_2CH_2N$), 2.51 (s, 6H, $C_{imi}CH_3$), 2.36 (s, 6H, $C_{mes}CH_3$), 1.99 (s, 12H, $C_{mes}CH_3$). ^{13}C{^{1}H} NMR (CD_3CN, 125 MHz) δ 146.2 (NCN), 142.3 ($C_{mes}CH_3$), 136.1 ($C_{mes}CH_3$), 131.3 (C_{mes}N), 130.6 (C_{mes}H), 123.6 (C_{imi}), 123.3 (C_{imi}), 46.6 ($NCH_2CH_2CH_2N$), 30.9 ($NCH_2CH_2CH_2N$), 21.1 ($C_{mes}CH_3$), 17.6 ($C_{mes}CH_3$), 10.8 ($C_{imi}CH_3$). Anal. calc. for $C_{29}H_{38}Br_2N_4$ (602.45) × 2 CH_3CN: C, 57.90; H, 6.48; N, 12.28. Found: C, 57.92; H, 6.40; N, 12.28.

Spectroscopic data for 2a

The monometallic species **2a** was obtained by dissolving complex **3a** in MeCN. Two species are distinguishable in the NMR spectra in a 2:1 ratio. *Major species:* ^{1}H NMR (CD_3CN, 500 MHz): δ 7.60 (m, 6H, H_{aryl}), 7.42 (d, 4H, $^3J_{HH}$ = 8.0 Hz, H_{aryl}), 7.08 (br, 2H, H_{imi}), 4.22 (m, 2H, NCHHCHCHHN), 3.83 (m, 5H, RhCH + NCH_2CH$_2$CH$_2$CH$_3$), 3.49 (m, 2H, NCH*H*CHCH*H*N), 1.61 (quintet, 4H, $^3J_{HH}$ = 7.5 Hz, NCH$_2$CH_2CH$_2$CH$_3$), 1.14 (sextet, 4H, $^3J_{HH}$ = 7.5 Hz, NCH$_2$CH$_2$CH_2CH$_3$), 0.76 (t, 6H, $^3J_{HH}$ = 7.5 Hz, NCH$_2$CH$_2$CH$_2$CH_3). *Minor species:* ^{1}H NMR (CD_3CN, 500 MHz): δ 7.60 (m, 6H, H_{aryl}), 7.46 (dd, 4H, $^3J_{HH}$ = 8.0 Hz, $^4J_{HH}$ = 1.5 Hz, H_{aryl}), 6.93 (s, 2H, H_{imi}), 4.22 (m, 2H, NC*H*HCHC*H*HN), 3.83 (m, 4H, NCH_2CH$_2$CH$_2$CH$_3$), 3.72 (m, 1H, RhCH), 3.49 (m, 2H, NCH*H*CHCH*H*N), 1.66 (quintet, 4H, $^3J_{HH}$ = 7.5 Hz, NCH$_2$CH_2CH$_2$CH$_3$), 1.14 (sextet, 4H, $^3J_{HH}$ = 7.5 Hz, NCH$_2$CH$_2$CH_2CH$_3$), 0.79 (t, 6H, $^3J_{HH}$ = 7.5 Hz, NCH$_2$CH$_2$CH$_2$CH_3). ^{13}C{^{1}H} NMR (CD_3CN, 125 MHz): δ 132.0 (C_{aryl}H), 130.5 (C_{aryl}H), 130.2 (C_{aryl}H), 121.8 (C_{imi}), 106.2 (C_{aryl}), 59.4 (N*C*H$_2$CH*C*H$_2$N), 48.0 (N*C*H$_2$CH$_2$CH$_2$CH$_3$), 33.0 (NCH$_2$*C*H$_2$CH$_2$CH$_3$), 20.1 (NCH$_2$CH$_2$*C*H$_2$CH$_3$), 13.6 (NCH$_2$CH$_2$CH$_2$*C*H$_3$). The carbene carbon, NCN and RhCH signals are not resolved in the ^{13}C{^{1}H} spectrum. The signals of the major and minor species differ by less than 0.3 ppm.

Spectroscopic data for 2b

The monometallic species **2b** was obtained by dissolving complex **3b** in MeCN. Two species are distinguishable in the ^{1}H NMR spectrum in a 1.2:1 ratio. *Major species:* ^{1}H NMR (CD_3CN, 360 MHz): δ 7.09, 7.04 (2 × s, 2H, H_{mes}), 6.55 (s, 2H, H_{imi}), 4.43 (br, 2H, NC*H*HCHC*H*HN), 4.04 (br, 1H, RhCH), 3.90 (m, 2H, NCH*H*CHCH*H*N) 2.33 (s, 6H, $C_{imi}CH_3$), 2.19 (s, 6H, $C_{mes}CH_3$), 1.98 (s, 6H, $C_{mes}CH_3$), 1.75 (s, 6H, $C_{mes}CH_3$). *Minor species:* ^{1}H NMR (CD_3CN, 360 MHz): δ 7.07, 7.02 (2 × s, 2H, H_{mes}), 6.69, 6.40 (2 × br, 2H, H_{imi}), 4.35 (m, 2H, NC*H*HCH$_2$C*H*HN), 3.90 (m, 3H, RhCH + NCH*H*CHCH*H*N), 2.32 (s, 6H, $C_{imi}CH_3$), 2.14 (br, 6H, $C_{mes}CH_3$), 1.96 (br, 6H, $C_{mes}CH_3$), 1.73 (br, 6H, $C_{mes}CH_3$). ^{13}C{^{1}H} NMR (CD_3CN, 125 MHz): δ 146.0 ($^1J_{RhC}$ = 46.2 Hz, C_{imi}), 141.2 (s, NCN), 136.1 (*C*$_{mes}$CH$_3$), 132.3 (*C*$_{mes}$CH$_3$), 130.1 (C_{mes}), 120.9 (d, $^2J_{RhC}$ = 2.9 Hz, C_{imi}), 59.0 (N*C*H$_2$CH*C*H$_2$N), 34.0 (d, $^1J_{RhC}$ = 28.5 Hz, RhCH), 21.0 (C_{imi}*C*H$_3$) 17.4, 17.3, 11.0 (3 × C_{mes}*C*H$_3$). The C_{mes}N signal is not well resolved in the ^{13}C{^{1}H} spectrum. The signals of the major and minor species differ by less than 0.3 ppm.

Synthesis of 3a

Compound **1a** (301 mg, 0.5 mmol), $RhCl_3.H_2O$ (132 mg, 0.5 mmol) and NaOAc (328 mg, 4.0 mmol) were stirred in refluxing MeCN (30 mL) for 16 h. Then KI (332 mg, 2.0 mmol) was added and stirring at reflux was continued for a further hour. The reaction mixture was cooled to room temperature and all volatiles were removed under reduced pressure. The residue was purified by column chromatography (SiO_2; CH_2Cl_2/acetone, 5:2), thus affording **3a** as a brown solid (0.24 g, 60%). Two major sets of signals are distinguishable in the NMR spectra in an approximate 2:1 ratio. ^{1}H NMR (CD_2Cl_2, 500 MHz): δ 7.61–7.53 (m, 6H, H_{aryl}), 7.36–7.30 (m, 4H, H_{aryl}), 7.02, 6.93, 6.92 (s, 2H, H_{imi}), 4.60–4.14 (m, 3H, RhCH + NC*H*HCHC*H*HN), 3.89–3.68 (m, 4H, NCH_2CH$_2$CH$_2$CH$_3$), 3.67–3.46 (m, 2H, NCH*H*CHCH*H*N), 1.77–1.66 (m, 4H, NCH$_2$CH_2CH$_2$CH$_3$), 1.25–1.18 (m, 4H, NCH$_2$CH$_2$CH_2CH$_3$), 0.84, 0.83, 0.82 (t, $^3J_{HH}$ = 7.0 Hz, 6H, NCH$_2$CH$_2$CH$_2$CH_3). ^{13}C{^{1}H} NMR (CD_2Cl_2, 125 MHz): 140.0 (NCN), 131.7, 131.6 (2 × C_{aryl}H), 130.1, 130.0 (2 × C_{aryl}H), 129.75 (C_{aryl}H), 125.2 (C_{aryl}), 122.1, 121.3 (2 × C_{imi}), 61.6 (N*C*H$_2$CH*C*H$_2$N), 48.7, 48.1 (2 × N*C*H$_2$CH$_2$CH$_2$CH$_3$), 38.5 ($^1J_{RhC}$ = 29.6 Hz, RhCH), 32.9, 32.7 (NCH$_2$*C*H$_2$CH$_2$CH$_3$), 20.3, 20.2 (2 × NCH$_2$CH$_2$*C*H$_2$CH$_3$), 14.0, 13.8 (2 × NCH$_2$CH$_2$CH$_2$*C*H$_3$). The carbene carbon signal is not well resolved in the ^{13}C{^{1}H} spectrum. Anal. calc. for $C_{58}H_{70}I_4N_8Rh_2$ (1592.66) × CH_2Cl_2: C, 40.89; H, 4.23; N, 6.36. Found: C, 40.91; H, 4.30; N, 6.57.

Synthesis of 3b

According to the procedure described for **3a**, complex **3b** was produced from **1b** (277 mg, 0.4 mmol), $RhCl_3.H_2O$ (105 mg, 0.4 mmol), NaOAc (263 mg, 3.2 mmol) and KI (266 mg, 1.6 mmol) as a brown solid (189 mg, 74%). Two major sets of signals are distinguishable in the NMR spectra in an approximate 2:1 ratio. ^{1}H NMR (CD_2Cl_2, 500 MHz): δ 7.05–6.91 (s, 4H, H_{mes}), 6.65, 6.63, 6.63 (s, 2H, H_{imi}), 4.67–4.58 (m, 1H, RhCH), 4.58–4.41 (m, 2H, NC*H*HCHC*H*HN), 3.94–3.81 (m, 2H, NCH*H*CHCH*H*N), 2.33, 2.32 (s, 6H, $C_{imi}CH_3$), 2.18 (s, 6H, $C_{mes}CH_3$), 1.99 (s, 6H, $C_{mes}CH_3$), 1.75, 1.72 (s, 6H, $C_{mes}CH_3$). ^{13}C{^{1}H} NMR (CD_2Cl_2, 125 MHz): δ 140.6 (NCN), 135.5 (br, *C*$_{mes}$CH$_3$), 132.1 (br, *C*$_{mes}$CH$_3$), 129.9, 129.8 (2 × C_{mes}), 121.7 (br, C_{imi}), 60.52, 60.17 (2 × N*C*H$_2$CH*C*H$_2$N), 37.7 (d, $^1J_{RhC}$ = 32.0, RhCH), 21.4 (C_{imi}*C*H$_3$), 17.5 (C_{mes}*C*H$_3$), 10.6 (C_{mes}*C*H$_3$). The carbene carbon signal and C_{mes}N signals are not well resolved in the ^{13}C{^{1}H} spectrum. Anal. calc. for $C_{58}H_{70}I_4N_8Rh_2$ (1592.67) × CH_2Cl_2: C, 42.24; H, 4.33; N, 6.68. Found: C, 42.16; H, 4.73; N, 6.61.

Synthesis of 4.

According to the general procedure described for **2a-b**, starting from **1e** (353 mg, 0.74 mmol), $RhCl_3.H_2O$ (194 mg, 0.74 mmol), NaOAc (484 mg, 5.9 mmol) and KI (490 mg, 3.0 mmol). The crude product was purified by column chromatography (SiO_2). Complex **5** was eluted selectively with CH_2Cl_2/acetone (5:2), and a mixture of complexes **4**, **5**, **6** and some monocarbene species were obtained as a brown solid by increasing the polarity of the mobile phase (CH_2Cl_2/acetone 5:3). Gradient column chromatography followed by fractional crystallisation induced by slow diffusion of Et_2O into a solution of the crude mixture of **4** and **6** in CH_3CN and acetone (1:1) gave two different types of crystals that were manually separated. Complex **4** crystallised as red rods, complex **6** as yellowish needles. ^{1}H NMR (CD_3CN, 600 MHz, 333 K): δ 8.31, 7.07, 6.91, 6.86 (4 × s, 1H, H_{imi}), 4.38 (br, 1H, NC*H*HCHCH$_2$N), 4.32 (dd, 1H, $^2J_{HH}$ = 12.0 Hz, $^3J_{HH}$ = 7.7 Hz, NCH$_2$CHC*H*HN), 4.21 (br, 3H, RhCH + NCH_2CH$_2$CH$_2$CH$_3$), 3.97 (t, 2H, NCH_2CH$_2$CH$_2$CH$_3$), 3.83 (d, 1H, $^2J_{HH}$ = 13.0 Hz, NCH*H*CHCH$_2$N), 3.67 (d, 1H, $^2J_{HH}$ = 12.0 Hz, NCH$_2$CHCH*H*N), 1.80 (m, 2H, NCH$_2$CH_2CH$_2$CH$_3$), 1.75 (quintet, 2H, $^3J_{HH}$ = 7.3 Hz, NCH$_2$CH_2CH$_2$CH$_3$), 1.38 (sextet, 2H, $^3J_{HH}$ = 6.0 Hz, NCH$_2$CH$_2$CH_2CH$_3$), 1.26 (m, 2H, NCH$_2$CH$_2$CH_2CH$_3$), 0.98, 0.90 (2 × t, 3H, $^3J_{HH}$ = 7.4 Hz, NCH$_2$CH$_2$CH$_2$CH_3). ^{13}C{^{1}H} NMR (CD_3CN, 150 MHz): δ 132.2, 122.6, 121.6, 119.5 (4 × C_{imi}), 60.7, 60.4 (2 ×

N*C*H_2CH*C*H_2N), 49.8, 49.4 (2 × N*C*H_2CH$_2$CH$_2$CH$_3$), 35.5 (RhCH), 33.7, 33.0 (2 × NCH$_2$*C*H$_2$CH$_2$CH$_3$), 20.6, 20.1 (2 × NCH$_2$CH$_2$*C*H$_2$CH$_3$), 14.2, 13.7 (2 × NCH$_2$CH$_2$CH$_2$*C*H$_3$). The carbene carbon signals are not well resolved in the $^{13}C\{^1H\}$ spectrum. Anal calc. for $C_{21}H_{33}I_2N_6Rh$ (726.24): C, 34.73; H, 4.58; N, 11.57. Found: C, 34.76; H, 4.53; N, 11.73.

Synthesis of 6.

Method A: According to the procedure described for the synthesis of complex **4**.

Method B: Complex **5** (80 mg, 0.16 mmol) and NaOAc (107 mg, 1.3 mmol) were stirred together in refluxing acetonitrile (20 mL) for 6 days. Solid KI (224 mg, 1.6 mmol) was added and the reaction mixture refluxed for 2 more days. The product was purified by column chromatography (SiO_2, CH_2Cl_2/acetone first 10:1, then 10:3) and **6** was obtained as a yellow solid (26 mg, 23% yield) after solvent removal. ^1H NMR (CD_3CN, 500 MHz, 343 K): δ 7.15, 7.03 (2 × s, 1H, H_{imi}), 4.56 (br, 1H, RhCH), 4.35 (m, 4H, NC*H*HCHC*H*HN + NC*H*HCH$_2$CH$_2$CH$_3$), 4.06 (m, 2H, NCH*H*CH$_2$CH$_2$CH$_3$), 3.67 (m, 2H, NCH*H*CHCH*H*N), 1.87, 1.79 (2 × m, 2H, NCH$_2$C*H$_2$*CH$_2$CH$_3$), 1.40 (sextet, 4H, $^3J_{HH}$ = 7.4 Hz, NCH$_2$CH$_2$C*H$_2$*CH$_3$), 0.98 (t, 6H, $^3J_{HH}$ = 7.3 Hz, NCH$_2$CH$_2$CH$_2$C*H$_3$*). $^{13}C\{^1H\}$ NMR (CD_3CN, 125 MHz): δ 123.0, 122.9, 120.4, 120.2 (4 × C_{imi}), 60.4, 60.1 (2 × N*C*H$_2$CH*C*H$_2$N), 50.1, 49.8 (2 × N*C*H$_2$CH$_2$CH$_2$CH$_3$), 36.0 (RhCH), 33.9, 33.3 (2 × NCH$_2$*C*H$_2$CH$_2$CH$_3$), 20.6, 20.4 (2 × NCH$_2$CH$_2$*C*H$_2$CH$_3$), 14.1 (NCH$_2$CH$_2$CH$_2$*C*H$_3$). Carbene carbon signal not resolved. Anal. Calc. for $C_{19}H_{30}I_2N_5Rh$ (685.19): C, 33.31; H, 4.41; N, 10.22. Found: C, 33.32; H, 4.14; N, 10.61.

Structure determination and refinement of 3b, 4, 5b and 6.

Suitable single crystals were mounted on Stoe Imaging Plate Diffractometer Systems[36] with a two-circle goniometer (**3b** and **4**) or a one-circle φ goniometer (**5b**), or on a Bruker SMART APEX CCD diffractometer (**6**). Graphite-monochromators (Mo-Kα radiation, λ = 0.71073 Å). For **3b** and **4**, a semi-empirical absorption correction was applied using MULscanABS as implemented in PLATON.[37] An empirical absorption correction was applied for **6** using the SADABS routine,[38] and no absorption correction was applied for **5b**. The structures were solved by direct methods using the program SHELXS-97[39] and refined by full matrix least squares on F^2 with SHELXL-97. The hydrogen atoms were included in calculated positions and treated as riding atoms using SHELXL-97 default parameters. All non-hydrogen atoms were refined anisotropically.

Crystals of complex **3b** contained one half-occupied CH_2Cl_2 per complex molecule. Disorder was found in one mesityl substituent and in the PF_6^- anion, and more pronounced in the co-crystallised solvent molecules. The SQUEEZE option in PLATON was used to calculate the potential solvent accessible volume (1848 Å, containing about 385 electrons). Eight hexane molecules (8 × 50 electrons) per unit cell were included in all further calculations. Due to the disorder, the corresponding parts of the ligand were refined as having the same thermal values. Compound **5b** crystallised as a racemic twin, therefore the TWIN refinement was applied in SHELXL. For **6**, the absolute structure was determined, the final Flack parameter is –0.03(3). Further details on data collection and refinement are summarised in Table S1.† Crystallographic data (excluding structure factors) have been deposited with the Cambridge Crystallographic Centre as supplementary publication nos. CCDC 817392–817395. Copies of the data can be obtained free of charge on application to CCDC, 12 Union Road, Cambridge CB2 1EZ, UK [fax: +44-1223-336-033; e-mail: deposit@ccdc.cam.ac.uk].

Acknowledgements

We thank F. Fehr, Y. Ortin, and J. Muldoon, for analytical assistance and the Swiss National Science Foundation, the Alfred Werner Foundation, and Sasol Ltd for financial support of this work.

Notes and references

[a] *School of Chemistry and Chemical Biology, University College Dublin, Belfield, Dublin 4, Ireland. Fax: +353-17162501; Tel: +353-17162504; martin.albrecht@ucd.ie*
[b] *School of Engineering and Physical Sciences, William Perkin Building, Heriot-Watt University, Edinburgh, EH14 4AS, U.K. E-mail: s.a.macgregor@hw.ac.uk*
[c] *XRD Application Lab, CSEM, Rue Jaquet-Droz 1, CH-2002 Neuchâtel, Switzerland*

† Electronic Supplementary Information (ESI) available: Crystallographic and computational details and computed structures and energies of all species. See DOI: 10.1039/b000000x/

1 (*a*) R. Jazzar, J. Hitce, A. Renaudat, J. Sofack-Kreutzer and O. Baudoin, *Chem. Eur. J.*, 2010, **16**, 2654. (*b*) R. Giri, B.-F. Shi, K. M. Engle, N. Maugel and J.-Q. Yu, *Chem. Soc. Rev.*, 2009, **38**, 3242.
2 M. S. Chen and M. C. White, *Science*, 2007, **318**, 783.
3 (*a*) V. Vidal, A. Theolier, J. Thivolle-Cazat and J.-M. Basset, *Science,* 1997, **276**, 99. (*b*) A. S. Goldman, A. H. Roy, Z. Huang, R. Ahuja, W. Schinski and M. Brookhart, *Science*, 2006, **312**, 257.
4 (*a*) R. H. Crabtree, *Chem. Rev.*, 1985, **85**, 245. (*b*) A. E. Shilov and G. B. Shul'pin, *Russ. Chem. Rev.*, 1987, **56**, 442. (*c*) B. A. Arndtsen and R. G. Bergman, *Science*, 1995, **270**, 1970. (*d*) J. Corker, F. Lefebvre, C. Lecuyer, V. Dufaud, F. Quignard, A. Choplin, J. Evans and J.-M. Basset, *Science,* 1996, **271**, 966. (*e*) R. A. Periana, O. Mironov, D. Taube, G. Bhalla and C. J. Jones, *Science*, 1998, **280**, 560. (*f*) J. A. Labinger and J. E. Bercaw, *Nature*, 2002, **417**, 507. (*g*) A. S. Goldman and K. I. Goldberg (Eds.), *Activation and Functionalization of C–H Bonds*, ACS Symposium Series 885, Wiley (Washington, D.C.) 2004. (*h*) R. H. Crabtree, *J. Organomet. Chem*., 2004, **689**, 4083. (*i*) R. G. Bergman, *Nature*, 2007, **446**, 391. (*j*) J. F. Hartwig, *Nature*, 2008, **455**, 314. (*k*) C. Coperet, *Chem. Rev.*, 2010, **110**, 656–680. (*l*) J. Choi, A. MacArthur, M. Brookhart and A. S. Goldman, *Chem. Rev.*, 2011, **111**, 1761. For intramolecular processes, see *e.g.* ref 1a and (*m*) D. Lapointe and K. Fagnou, *Chem. Lett.*, 2010, **39**, 1119.
5 H. Arakawa, M. Aresta, J. N. Armor, M. A. Barteau, E. J. Beckman, A. T. Bell, J. E. Bercaw, C. Creutz, E. Dinjus, D. A. Dixon, K. Domen, D. L. DuBois, J. Eckert, E. Fujita, D. H. Gibson, W. A. Goddard, D. W. Goodman, J. Keller, G. J. Kubas, H. H. Kung, J. E. Lyons, L. E. Manzer, T. J. Marks, K. Morokuma, K. M. Nicholas, R. Periana, L. Que, J. Rostrup-Nielson, W. M. H. Sachtler, L. D. Schmidt, A. Sen, G. A. Somorjai, P. C. Stair, B. R. Stults and W. Tumas, *Chem. Rev*., 2001, **101**, 953.
6 Z. Lin, *Coord. Chem. Rev.*, 2007, **251**, 2280.
7 R. N. Perutz and S. Sabo-Etienne, *Angew. Chem., Int. Ed.,* 2007, **46**, 2578.

8 (*a*) A. Dedieu, *Chem. Rev.*, 2000, **100**, 543. (*b*) S. Sakaki, *Top. Organomet. Chem.*, 2005, **12**, 31. (*c*) M. Lersch, M. Tilset, *Chem. Rev.*, 2005, **105**, 2471.

9 (*a*) H. Chen, S. Schlecht, T. C. Semple and J. F. Hartwig, *Science*, 2000, **287**, 1995. (*b*) I. A. I. Mkhalid, J. H. Barnard, T. B. Marder, J. M. Murphy and J. F. Hartwig, *Chem. Rev.*, 2010, **110**, 890.

10 In this context, electrophilic metals imply a larger charge transfer from the C–H bond to the metal, whereas nucleophilic centres engage in larger backbonding, *i.e.* charge transfer from the metal to the C–H σ^* orbital. In amphiphilic centres bonding and backbonding are nearly balanced. See: D. H. Ess, W. A. Goddard, R. A. Periana, *Organometallics*, 2010, **29**, 6459.

11 (*a*) Y. Boutadla, D. L. Davies, S. A. Macgregor and A. I. Poblador-Bahamonde, *Dalton Trans*., 2009, 5820. (*b*) C. E. Kefalidis, O. Baudoin and E. Clot, *Dalton Trans*., 2010, **39**, 10528. (*c*) D. Balcells, E. Clot and O. Eisenstein, *Chem. Rev.* 2010, **110**, 749.

12 (*a*) D. Bourissou, O. Guerret, F. P. Gabbaie and G. Bertrand, *Chem. Rev.*, 2000, **100**, 39. (*b*) W. A. Herrmann, *Angew. Chem., Int. Ed.*, 2002, **41**, 1290. (*c*) F. E. Hahn and M. C. Jahnke, *Angew. Chem., Int. Ed.*, 2008, **47**, 3122. (*d*) S. Diez-Gonzalez, N. Marion and S. P. Nolan, *Chem. Rev.*, 2009, **109**, 3612. (*e*) L. Mercs and M. Albrecht, *Chem. Soc. Rev.*, 2010, **39**, 1903.

13 Intermolecular C–H bond activation: (*a*) M. Muehlhofer, T. Strassner and W. A. Herrmann, *Angew. Chem., Int. Ed.*, 2002, **41**, 1745. For examples of intramolecular C–H bond activation, see: (*b*) J. Huang, E. D. Stevens, S. P. Nolan, *Organometallics*, 2000, **19**, 1194. (*c*) R. Dorta, E. D. Stevens and S. P. Nolan, *J. Am. Chem. Soc.*, 2004, **126**, 5054. (*d*) S. Burling, B. M. Paine, D. Nama, V. S. Brown, M. F. Mahon, T. J. Prior, P. S. Pregosin, M. K. Whittlesey and J. M. J. Williams, *J. Am. Chem. Soc.*, 2007, **129**, 1987. (*e*) V. Lavallo and R. H. Grubbs, *Science*, 2009, **326**, 559. C–C bond activation: (*f*) R. F. R. Jazar, S. A. Macgregor, M. F. Mahon, S. P. Richards and M. K. Whittlesey, *J. Am. Chem. Soc.*, 2002, **124**, 4944. C–F bond activation: (*g*) V. P. W. Böhm, C. W. K. Gstöttmayr, T. Weskamp and W. A. Herrmann, *Angew. Chem., Int. Ed.*, 2001**, 40**, 3387.

14 (*a*) A. R. Chianese, A. Kovacevic, B. M. Zeglis, J. W. Faller, R. H. Crabtree, *Organometallics*, 2004, **23**, 2461. (*b*) M. Heckenroth, A. Neels, M. G. Garnier, P. Aebi, A. W. Ehlers, M. Albrecht, *Chem. Eur. J.*, 2009, **15**, 9375.

15 (*a*) P. L. Arnold and J. Pearson, *Coord. Chem. Rev.,* 2007, **251**, 596. (*b*) M. Albrecht, *Chem. Commun*., 2008, 3601. (*c*) O. Schuster, L. Yang, H. G. Raubenheimer and M. Albrecht, *Chem. Rev.,* 2009, **109**, 3445.

16 (*a*) M. Heckenroth, E. Kluser, A. Neels and M. Albrecht, *Angew. Chem., Int. Ed.*, 2007, **46**, 6293. (*b)* R. Lalrempuia, N. D. McDaniel, H. Mueller-Bunz, S. Bernhard and M. Albrecht, *Angew. Chem., Int. Ed.* 2010, **49**, 9765. (*c*) A. Prades, E. Peris and M. Albrecht, *Organometallics*, 2011, **30**, 1162. (*d*) A. Krüger and M. Albrecht, in *N-heterocyclic carbenes: From Laboratory Curiosities to Efficient Synthetic Tools*, ed. Silvia Diez-Gonzalez (Ed.), RSC (Cambridge, UK) 2011, p. 134.

17 A. Krüger, A. Neels and M. Albrecht, *Chem. Commun*., 2010, **46**, 315.

18 L. Yang, A. Krüger, A. Neels, M. Albrecht, *Organometallics,* **2008**, *27*, 3161.

19 (*a*) J. A. Mata, A. R. Chianese, J. R. Miecznikowski, M. Poyatos, E. Peris, J. W. Faller and R. H. Crabtree, *Organometallics*, 2004, **23**, 1253. (*b*) C. H. Leung, C. D. Incarvito and R. H. Crabtree, *Organometallics*, 2006, **25**, 6099.

20 (*a*) A. Pidcock, R. E. Richards and L. M. Venanzi, *J. Chem. Soc. A*, 1966, 1707. (*b*) R. Mason, R. McWeeny and A. D. C. Towl, *Faraday Discuss.*, 1969, **47**, 20. (*c*) R. G. Pearson, *Inorg. Chem.*, 1973, **12**, 712. (*d*) J. N. Harvey, K. M. Heslop, A. G. Orpen and P. G. Pringle, *Chem. Commun*., 2003, 278. (*e*) C. R. Landis, T. Cleveland and T. K. Firman, *J. Am. Chem. Soc.*, 1998, **120**, 2641.

21 (*a*) M. Albrecht, R. H. Crabtree, J. Mata and E. Peris, *Chem. Commun*., 2002, 32-33. (*b*) M. Poyatos, M. Sanau and E. Peris, *Inorg. Chem.*, 2003, **42**, 2572.

22 IUPAC. Compendium of Chemical Terminology, 2nd ed. (the "Gold Book") compiled by A. D. McNaught and A. Wilkinson, Blackwell Scientific Publications, Oxford, 1997.

23 E. Aldeco-Perez, A. J. Rosenthal, B. Donnadieu, P. Parameswaran, G. Frenking, G. Bertrand, *Science,* 2009, **326**, 556.

24 Exclusive arrangement of the iodide ligand *cis* to the alkyl ligand is in agreement with the a significantly different *trans* influence of the normal NHC and the alkyl ligand. Notably, this difference is considerably smaller between abnormal NHC and the alkyl group, *cf.* NMR spectroscopic data of **2** and **4**.

25 (*a*) W. A. Herrmann, J. Schwarz and M. G. Gardiner, *Organometallics*, 1999, **18**, 4082. (*b*) M. Heckenroth, E. Kluser, A. Neels and M. Albrecht, *Dalton Trans.,* 2008, 6242.

26 This conclusion is further supported by separate experiments involving the exposure of pure complex **4** or **6** to the reaction conditions used for their preparation (KI, NaOAc, MeCN, reflux for several hours). In either case, the complexes were stable and did not show any detectable interconversion to the other complex.

27 (*a*) A. M. Magill and B. F. Yates, *Aust. J. Chem.*, 2004, **51**, 1205. (*b*) A. M. Magill, K. J. Cavell and B. F. Yates, *J. Am. Chem. Soc.*, 2004, **126**, 8717.

28 C. E. Ellul, M. F. Mahon, O. Saker and M. K. Whittlesey, *Angew. Chem. Int. Ed.* **2007**, *46*, 6343.

29 (*a*) D. L. Davies, S. M. A. Donald and S. A. Macgregor, *J. Am. Chem. Soc*., 2005, **127**, 13754. (*b*) D. Garcia- Cuadrado, A. A. C. Braga, F. Maseras and A. M. Echavarren, *J. Am. Chem. Soc*., 2006, **128**, 1066. (*c*) D. L. Davies, S. M. A. Donald, O. Al-Duaij, J. Fawcett, C. Little and S. A. Macgregor, *Organometallics*, 2006, **25**, 5976. (*d*) D. Garcia-Cuadrado, P. de Mendoza, A. A. C. Braga, F. Maseras and A. M. Echavarren, *J. Am. Chem. Soc*., 2007, **129**, 6880. (*e*) S. I. Gorelsky, D. Lapointe and K. Fagnou, *J. Am. Chem. Soc*., 2008, **130**, 10848. (*f*) D. R. Stuart, M. Bertrand-Laperle, K. M. N. Burgess and K. Fagnou, *J. Am. Chem. Soc*., 2008, **130**, 16474. (*g*) Y. Boutadla, D. L. Davies, S. A. Macgregor and A. I. Poblador-Bahamonde, *Dalton Trans*., 2009, 5820. (*h*) M. Albrecht, *Chem. Rev.* 2010, **110**, 579.

30 Eclipsed interactions may also contribute to the observed reactivity differences. These would be expected to be more pronounced in C2-bound **A** rather than C4-bound $\mathbf{A_{ab}}$ because of the different position of N-substituents relative to the axial iodide ligand.

31 M. K. Denk and J. M. Rodezno, *J. Organomet. Chem.*, 2000, **608**, 122.

32 S. Gründemann, A. Kovacevic, M. Albrecht, J. W. Faller and R. H. Crabtree, *J. Am. Chem. Soc.*, 2002, **124**, 10476.

33 Despite that experiments were conducted under strictly anhydrous conditions, water as a proton source cannot be fully excluded.

34 For related ligand cooperativity, see: (*a*) D. B. Grotjahn, *Chem. Eur. J.,* 2005, **11**, 7146. (*b*) C. Gunanathan, Y. Ben-David and D. Milstein, *Science,* 2007, **317**, 790. (*c*) H. Grützmacher, *Angew. Chem., Int. Ed.,* 2008, **47**, 1814. (*d*) T. Zweifel, J.-V. Naubron and H. Grützmacher, *Angew. Chem., Int. Ed.,* 2009, **48**, 559.

35 A. A. Gridnev and I. M. Mihaltseva, *Synth. Commun.*, **1994**, *24*, 1547.

36 Stoe & Cie (2000). IPDS-I Bedienungshandbuch. Stoe & Cie GmbH, Darmstadt, Germany.

37 A. L. Spek, *J.Appl.Cryst.*, 2003, **36**, 7-13.

38 Bruker (2001). SADABS, Bruker AXS Inc., Madison, Wisconsin, USA.

39 G. M. Sheldrick, *Acta Cryst*. **2008**, *A64*, 112.

ToC entry

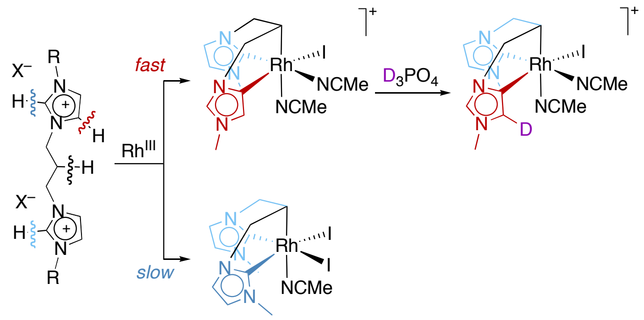

Strongly mesoionic imidazol-4-ylidene N-heterocyclic carbene ligands promote the rhodium-mediated activation of an alkane-type C–H bond and undergo H/D exchange via exclusive C5–H bond activation.